Two-dome superconductivity in FeS induced by a Lifshitz transition

Makoto Shimizu,[1] Nayuta Takemori,[1] Daniel Guterding,[2] and Harald O. Jeschke[1,*]

[1] *Research Institute for Interdisciplinary Science, Okayama University, Okayama 700-8530, Japan*
[2] *Institut für Theoretische Physik, Goethe-Universität Frankfurt, Max-von-Laue-Straße 1, 60438 Frankfurt am Main, Germany*

Among iron chalcogenide superconductors, FeS can be viewed as a simple, highly compressed relative of FeSe without nematic phase and with weaker electronic correlations. Under pressure, however, the superconductivity of stoichiometric FeS disappears and reappears, forming two domes. We perform electronic structure and spin fluctuation theory calculations for tetragonal FeS in order to analyze the nature of the superconducting order parameter. In random phase approximation we find a gap function with d-wave symmetry at ambient pressure, in agreement with several reports of a nodal superconducting order parameter in FeS. Our calculations show that as function of pressure, the superconducting pairing strength decreases until a Lifshitz transition takes place at 4.6 GPa. As a hole pocket with large density of states appears at the Lifshitz transition, the gap symmetry is altered to sign-changing s-wave. At the same time the pairing strength is severely enhanced and increases up to a new maximum at 5.5 GPa. Therefore, our calculations naturally explain the occurrence of two superconducting domes in FeS.

Introduction.– The structurally simplest class of iron-based superconductors with its prime representative FeSe [1] was discovered in the same year as LaFeAsO [2]. FeSe has been intensively studied due to its very large nematic region [3], its interesting magnetism [4] and the complexity of its electronic structure [5]. Only in 2015 was it established that the isostructural FeS is also a superconductor [6]. Even though the replacement of Se by the smaller S appears to be a minor structural modification, it soon became clear that FeSe and FeS behave differently in several respects: The nematic region is absent in FeS [7], the electronic correlations appear to be significantly smaller in FeS [8], and the upper critical field is much smaller [9]. In fact, the possibility to grow high quality mixed $FeSe_{1-x}S_x$ structures has provided opportunities to study the evolution of properties between FeSe and FeS [8, 10–13].

Superconductivity in FeS has been observed below $T_c = 5$ K [6] with some variation due to sample dependence [14]. Scanning tunneling spectroscopy points to strong-coupling superconductivity [15], and Hall conductivities can be fitted with a two-band model [16]. The symmetry of the superconducting gap in FeS has been the subject of some debate. Using scanning tunneling spectroscopy, Yang *et al.* [15] conclude that the superconducting gap of FeS is strongly anisotropic. Specific heat measurements [17] and quasiparticle heat transport studies [18] point to a nodal gap structure. However, muon spin rotation studies found fully gapped behavior in FeS [19, 20]. Theoretically, a $d_{x^2-y^2}$ order parameter at ambient pressure has been obtained [21].

Pressure has been shown to suppress superconductivity in FeS [22]. Surprisingly, however, Zhang *et al.* have found that after the initial suppression, at a pressure of $P = 5$ GPa superconductivity reemerges, and a second superconducting dome is formed, up to a pressure of $P = 22.3$ GPa. Such double dome superconductivity is known to occur also in alkali iron selenides [23] and in FeSe intercalates [24, 25]. In fact, two superconducting domes occur in nearly all classes of unconventional superconductors [26].

In this contribution, we consider the structurally simple FeS as an instructive example system for studying the origin of double dome superconductivity in iron-based materials. We show that at a pressure of $P = 4.6$ GPa, a Lifshitz transition occurs, adding a hole pocket to the Fermi surface and boosting the density of states at the Fermi level. Using spin fluctuation theory in the random phase approximation, we show that pairing strength of the $d_{x^2-y^2}$ order parameter, which dominates within the low pressure dome, decreases until a Lifshitz transition of the electronic structure takes place. At the transition, the superconducting order parameter switches to nodeless $s_\pm$, and the pairing strength grows significantly to a new maximum. Our study highlights that even without a structural phase transition, the pressure induced changes in the electronic structure trigger the reemergence of superconductivity in FeS.

Structure.– The metastable tetragonal structure of FeS ($P4/nmm$ space group) occurs as a mineral named mackinawite [27]. Single crystals can be synthesized by hydrothermal synthesis [6, 27] and by deintercalation of $K_xFe_{2-y}S_2$ [9]. We base our study on the pressure series of tetragonal crystal structures determined by Zhang *et al.* [28]. In this study, mackinawite is found to transform to the hexagonal troilite phase ($P\bar{6}2c$ space group) at high pressures, with a mixed region extending from 5 GPa to 9.2 GPa. However, the high pressure phase diagram of FeS is complicated, and orthorhombic ($Pnma$ space group) and monoclinic ($P2_1a$ space group) phases have also been described [22, 29].

Methods.– We perform density functional theory calculations for the tetragonal FeS structures within the full-potential local orbital (FPLO) [30] basis, using the gener-

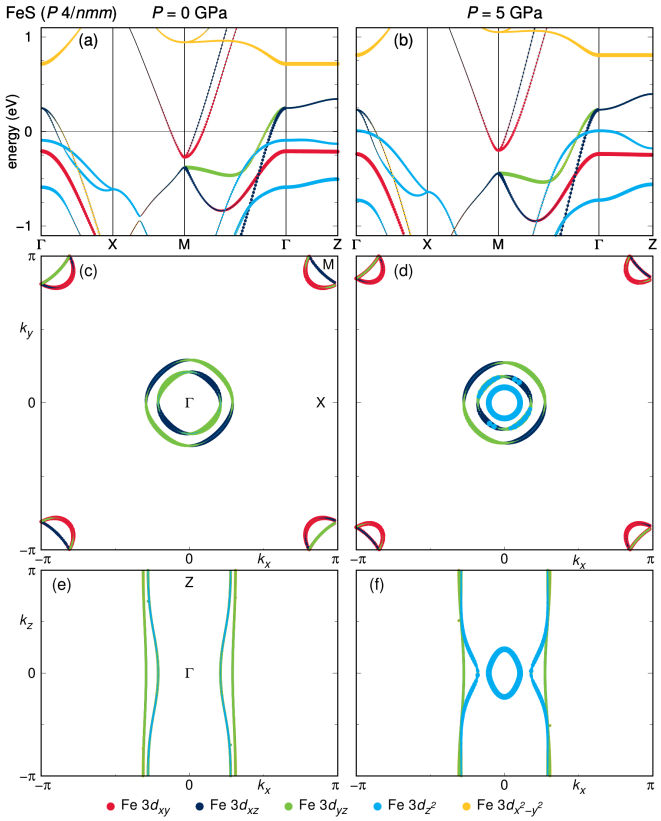

FIG. 1. Electronic structure of FeS at ambient pressure (left column) and at $P = 5$ GPa (right column). Band structures (a), (b), Fermi surfaces in the $k_x - k_y$ plane at $k_z = 0$ (c), (d) and Fermi surfaces in the $k_x - k_z$ plane (e), (f) are all colored with the orbital weights of the Fe $3d$ orbitals. A Lifshitz transition at $P = 4.6$ GPa adds a hole Fermi surface pocket near Γ.

alized gradient approximation (GGA) exchange correlation functional [31] and fine k meshes of $50 \times 50 \times 50$. We interpolate the experimental crystal structure (as shown in Ref. [35], Fig. S1), so that we can perform calculations employing fine pressure steps of 0.1 GPa. We construct ten band tight-binding models using the FPLO projective Wannier functions [32], including all Fe $3d$ states. We employ the unfolding method using point group symmetries [33] in order to obtain five band tight binding models. We study superconductivity assuming a spin-fluctuation driven pairing interaction within the multi-orbital Hubbard model and use the formalism as detailed by Graser *et al.* [34, 35] and as implemented in Refs. [36, 37]. We determine the non-interacting susceptibilities on $\mathbf{q}$ meshes of $50 \times 50 \times 10$ points at all pressures, and we use about 5000 k points on the Fermi surface for solving the gap equation in three dimensions; two-dimensional calculations are insufficient for FeS under pressure.

Results.– We first determine the electronic structure of tetragonal FeS in small pressure intervals up to a pressure of $P = 9.2$ GPa. Fig. 1 shows bands and Fermi surfaces at two representative pressures, $P = 0$ and $P = 5$ GPa. Our results at ambient pressure are in good agreement with angle resolved photoemission [38, 39] and quantum oscillation measurements [40]. The fact that FeS is rather weakly correlated [39] makes the plain GGA calculations a good starting point for our analysis of electronic structure and superconductivity. After a very smooth pressure evolution of the electronic structure, suddenly at $P = 4.6$ GPa a Lifshitz transition occurs and a hole pocket is added to the Fermi surface (Fig. 1 (b), (d), (f)). The reason for this event is the fact that the bands with Fe $3d_{z^2}$ orbital character widen more rapidly with pressure than the other iron bands. Careful analysis of the relationship between geometrical parameters in the FeS structure and its bands reveals that the $3d_{z^2}$ bands are especially sensitive to the Fe-S-Fe angle, much more so than to the Fe-S bond distance [35]. As a consequence, the $3d_{z^2}$ contribution to the density of states at the Fermi level $N(E_F)$ increases gradually below $P = 4.6$ GPa before it rises by more than 100% at the Lifshitz transition, as shown in Fig. 2(a).

We now consider the superconductivity in FeS, assuming a spin fluctuation induced Cooper pairing. We use the random phase approximation to calculate the spin susceptibility at all pressures (for details see Ref. [35]). In iron-based superconductors, the pairing interaction is often dominated by intra-orbital nesting (see f.i. Ref. [36]), and in particular χ^S_{xy} and χ^S_{yz} (or χ^S_{xz}), as shown in Figs. 2 (b) and (c), respectively. These elements of the spin susceptibility are diagonal in the four orbital indices, since we first investigate only intra-orbital contributions. The dominant peak in χ^S_{xy} is near a nesting vector $\mathbf{q} = (\pi, \pi)$, in χ^S_{yz} near $\mathbf{q} = (\pi, 0)$. In fact, these nesting vectors can also be extracted easily from a plot of the Fermi surface (Fig. 3).

For repulsive interaction, a peak in the spin susceptibility at vector $\mathbf{q}$ induces a sign change of the superconducting gap between Fermi surface pockets connected by $\mathbf{q}$. From the spin susceptibility, it is clear that the electronic structure of FeS leads to the competition between different order parameters, which is typical for iron-based superconductors. The peak at $\mathbf{q} = (\pi, 0)$ in χ^S_{yz} favors a sign change between hole cylinders around Γ and electron cylinders at X and Y, *i.e.* a type of sign changing s-wave order parameter, where the gap has the same sign on all electron pockets. On the other hand, the strong $\mathbf{q} = (\pi, \pi)$ peak in χ^S_{xy} favors a sign change between the electron pockets; this is most easily fulfilled by a $d_{x^2-y^2}$ order parameter. As a compromise between these two possibilities, a nodal sign changing s-wave order parameter sometimes occurs (see f.i. Ref. [36]).

Because of the increased band width and smaller density of states at the Fermi level, the spin susceptibility generally decreases with increasing pressure (Fig. 2(b) and (c)). Therefore, we find a general decline of pair-

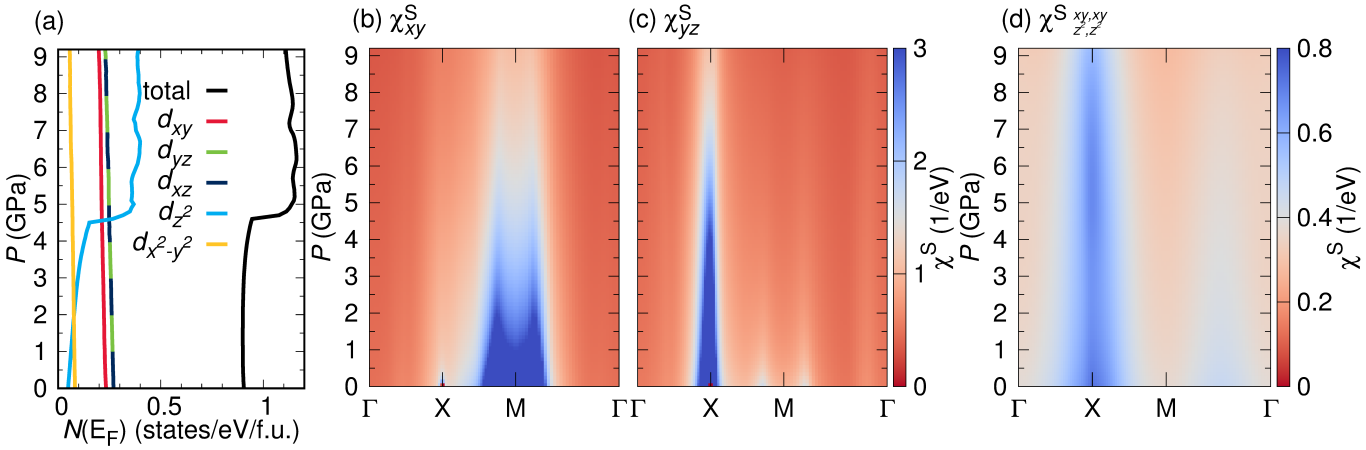

FIG. 2. Pressure dependence of (a) density of states at the Fermi level and (b), (c) diagonal elements and (d) off-diagonal elements of the spin susceptibility for tetragonal FeS.

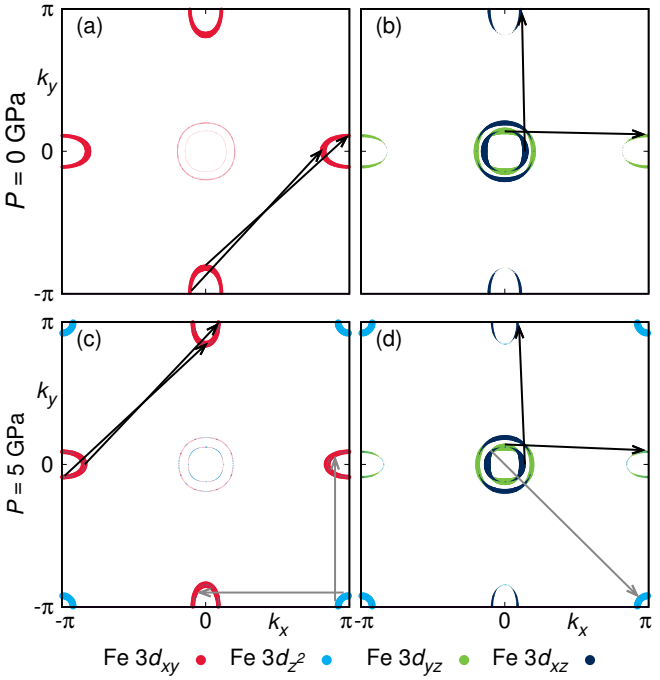

FIG. 3. Fermi surfaces in the one-iron Brillouin zone at $k_z = 0$ at ambient pressure and at $P = 5$ GPa (after the Lifshitz transition). Black arrows indicate important intra-orbital nesting vectors, gray arrows significant inter-orbital nesting vectors.

ing strength with increasing pressure (Fig. 4(b)). From a quantitative solution of the superconducting gap equation, we find (Fig. 4 (a)) that at $P = 0$, the $d_{x^2-y^2}$ solution wins, while several $s_\pm$ solutions are in competition, but subleading (Fig. 4 (b)). This result is in agreement with Ref. [21]. As a function of pressure, the eigenvalues of the gap equation are suppressed rapidly. Initially, no change in the symmetry of the superconducting gap is found. This corresponds well to the first superconducting dome that was observed experimentally [28].

However, very close to the Lifshitz transition, the nature of the superconducting order parameter changes dramatically. At $P = 4.65$ GPa, a new sign changing s type order parameter appears (Fig. 4 (c)) and becomes the dominating solution up to the highest pressure $P = 9.2$ GPa, at which the tetragonal phase is completely replaced by the hexagonal phase of FeS. The eigenvalue of the gap equation increases rapidly for this solution, in very good agreement to experiment, up to a maximum at $P = 5.4$ GPa. Thus, our calculation provides clear evidence for the existence of two dome superconductivity in FeS under pressure.

Note that the eigenvalue of the nodal $s_\pm$ solution is also enhanced at the Lifshitz transition, while the eigenvalue of the $d_{x^2-y^2}$ solution is not affected at all (Fig. 4(b)). This is the case, because the symmetry-required nodes of the $d_{x^2-y^2}$ solution are located exactly where the d_{z^2} hole pocket emerges. Therefore, it is naturally excluded from the $d_{x^2-y^2}$ solution.

As we have not studied superconductivity in the hexagonal phase, which is presumably of nonmagnetic, BCS origin, we cannot complete the second superconducting dome at the higher pressures investigated experimentally.

Discussion.– So far, we have demonstrated two important effects that occur in pressurized FeS without any structural discontinuity: A Lifshitz transition which creates a hole pocket and significant Fe $3d_{z^2}$ weight at the Fermi level, and a change of superconducting order parameter from d to sign-changing s-wave, which occurs at almost exactly the same pressure. The important question of the connection between the two events remains to be answered.

While the noninteracting diagonal susceptibility $\chi^0_{d_{z^2}}$ acquires some weak maximum near $\mathbf{q} = 0$ (see Ref. [35]), the diagonal spin susceptibility $\chi^S_{d_{z^2}}$ is nearly featureless and does not help to explain any change in superconduct-

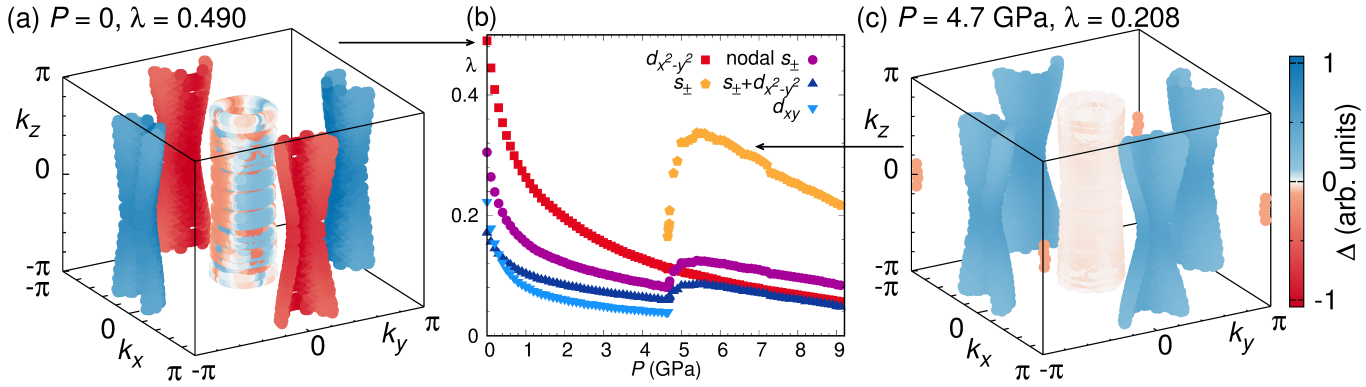

FIG. 4. Leading gap functions for FeS at (a) ambient pressure and (c) $P = 4.7$ GPa. The three-dimensional Fermi surfaces are plotted in the one-iron Brillouin zone. (b) Leading eigenvalues λ of the linearized gap equation as function of pressure. Up to $P = 4.6$ GPa, the $d_{x^2-y^2}$ order parameter dominates, but its eigenvalue decreases, marking the right half of the first superconducting dome. At the Lifshitz transition pressure $P = 4.6$ GPa, an $s_\pm$ solution takes over, with its eigenvalue forming a second superconducting dome.

ing order parameter. Note, that the hole Fermi surface around M in the unfolded one-iron Brillouin zone (see Fig. 4 (c)) is of different nature from the γ Fermi surface feature at M described in Ref. [41]; in their case, electron doping populates a pocket of d_{xy} orbital character (in the local coordinates chosen for the present analysis), and the pocket can contribute to pairing via the $\mathbf{q} = (\pi, \pi)$ peak in χ^S_{xy}.

Our case highlights the importance of the interaction terms proportional to U', J and J': They mediate participation of the d_{z^2} orbital in the pairing via the off-diagonal components of the spin susceptibility, such as $\chi^{S}{}^{bb}_{aa}$, $\chi^{S}{}^{ba}_{ab}$ and $\chi^{S}{}^{ab}_{ab}$ with $a = d_{z^2}$ and $b = d_{xy}$ (or in principle also $b = d_{xz/yz}$) (see Fig. 2(d) and Ref. [35]), which are significantly peaked at $\mathbf{q} = (\pi, 0)$. The inter-orbital nesting between d_{z^2} and d_{xz} is much weaker and does not contribute significantly to the pairing. Fig. 3 shows the relevant intra- and inter-orbital nesting vectors before and after the Lifshitz transition. This figure indeed confirms that there is considerable inter-orbital nesting between the d_{xy} and d_{z^2} orbitals.

Although Figs. 3(c) and (d) show that there is only a small pocket of d_{z^2} character, its strong influence on the pairing interaction is explained by the extremely large density of states at the Fermi level in this orbital after the Lifshitz transition (Fig. 2(a)).

Finally, we also comment on the negligible gap size on the central hole pockets in Fig. 4(c). The intra-orbital spin susceptibility of the $d_{xz/yz}$ orbitals, which is peaked at X, should lead to a sign change between the electron pockets and the central hole pockets as discussed before, with negative sign on the central hole pockets. However, the inter-orbital spin susceptibility between d_{z^2} and $d_{xz/yz}$, which is peaked at M, should lead to a sign change between the emergent hole-pocket and the central hole pockets, with positive sign on the central hole pockets. Therefore, these interactions are frustrated. As a compromise, the gap on the central hole pockets remains close to zero.

Since our analysis highlights the importance of inter-orbital interactions, one could expect that superconductivity breaks down once inter-orbital Coulomb interaction, Hund's rule coupling and pair-hopping term are neglected. We corroborate the significance of the inter-orbital interaction terms by solving the gap equation at finite intra-orbital Coulomb interaction $U = 1.9$ eV with other interactions set to zero ($U' = J = J' = 0$). The order parameter we obtain in this case is nodeless $s_\pm$, but, more importantly, the associated pairing eigenvalue is close to zero, *i.e.* superconductivity vanishes without inter-orbital interactions.

Conclusion.– We investigated the superconducting order parameter of tetragonal FeS using a combination of density functional theory calculations and spin fluctuation theory for the multi-orbital Hubbard model. We showed that a Lifshitz transition occurs in FeS at a pressure of about $P = 4.6$ GPa, which changes the superconducting order parameter from $d_{x^2-y^2}$ to a sign-changing s-wave, with significantly enhanced pairing strength right after the Lifshitz transition due to enhanced density of states at the Fermi level. While superconducting pairing within the first dome is dominated by intra-orbital nesting of d_{xy} states, the second dome features unusual inter-orbital nesting between d_{xy} and d_{z^2} states. In conclusion, our calculations explain the recently found double-dome superconductivity in FeS.

We acknowledge fruitful discussions with Seiichiro Onari and Kazuhiko Kuroki. N.T. is supported by JSPS KAKENHI Grant No. 16H07447. Part of the computations was carried out at the Supercomputer Center at the Institute for Solid State Physics, the University of Tokyo.

* jeschke@okayama-u.ac.jp

[1] F.-C. Hsu, J.-Y. Luo, K.-W. Yeh, T.-K. Chen, T.-W. Huang, P. M. Wu, Y.-C. Lee, Y.-L. Huang, Y.-Y. Chu, and D.-C. Yan, and M.-K. Wu, *Superconductivity in the PbO-type structure α-FeSe*, Proc. Natl. Acad. Sci. U.S.A. **105**, 14262 (2008).

[2] Y. Kamihara, T. Watanabe, M. Hirano, and H. Hosono, *Iron-Based Layered Superconductor La[$O_{1-x}F_x$]FeAs (x = 0.05-0.12) with T_c = 26 K*, J. Am. Chem. Soc. **130**, 3296 (2008).

[3] A. E Böhmer and A. Kreisel, *Nematicity, magnetism and superconductivity in FeSe*, J. Phys.: Condens. Matter **30**, 023001 (2018).

[4] J. K. Glasbrenner, I. I. Mazin, H. O. Jeschke, P. J. Hirschfeld, R.M. Fernandes, and R. Valentí, *Effect of magnetic frustration on nematicity and superconductivity in iron chalcogenides*, Nat. Phys. **11**, 953 (2015).

[5] A. Coldea and M. D. Watson, *The key ingredients of the electronic structure of FeSe*, Annu. Rev. Condens. Matter Phys. **9**, 125 (2018).

[6] X. Lai, H. Zhang, Y. Wang, X. Wang, X. Zhang, J. Lin, and F. Huang, *Observation of Superconductivity in Tetragonal FeS*, J. Am. Chem. Soc. **137**, 10148 (2015).

[7] M. D. Watson, T. K. Kim, A. A. Haghighirad, S. F. Blake, N. R. Davies, M. Hoesch, T. Wolf, A. I. Coldea, *Suppression of orbital ordering by chemical pressure in $FeSe_{1-x}S_x$*, Phys. Rev. B **92**, 121108 (2015).

[8] H. Man, J. Guo, R. Zhang, R. Schönemann, Z. Yin, M. Fu, M. B. Stone, Q. Huang, Y Song, W. Wang, D. J. Singh, F. Lochner, T. Hickel, I. Eremin, L. Harriger, J. W. Lynn, C. Broholm, L. Balicas, Q. Si and P. Dai, *Spin excitations and the Fermi surface of superconducting FeS*, npj Quant. Mater. **2**, 14 (2017).

[9] C. K. H. Borg, X. Zhou, C. Eckberg, D. J. Campbell, S. R. Saha, J. Paglione, E. E. Rodriguez, *Strong anisotropy in nearly ideal tetrahedral superconducting FeS single crystals*, Phys. Rev. B **93**, 094522 (2016).

[10] S. Hosoi, K. Matsuura, K. Ishida, H. Wang, Y. Mizukami, T. Watashige, S. Kasahara, Y. Matsuda, and T. Shibauchi, *Nematic quantum critical point without magnetism in $FeSe_{1-x}S_x$ superconductors*, Proc. Natl. Acad. Sci. **113**, 8139 (2016).

[11] K. Matsuura, Y. Mizukami, Y. Arai, Y. Sugimura, N. Maejima, A. Machida, T. Watanuki, T. Fukuda, T. Yajima, Z. Hiroi, K. Y. Yip, Y. C. Chan, Q. Niu, S. Hosoi, K. Ishida, K. Mukasa, T. Watashige, S. Kasahara, J.-G. Cheng, S. K. Goh, Y. Matsuda, Y. Uwatoko, T. Shibauchi, *Maximizing T_c by tuning nematicity and magnetism in $FeSe_{1-x}S_x$ superconductors*, Nat. Commun. **9**, 1143 (2017).

[12] Y. Sato, S. Kasahara, T. Taniguchi, X. Xing, Y. Kasahara, Y. Tokiwa, Y. Yamakawa, H. Kontani, T. Shibauchi, and Y. Matsuda, *Abrupt change of the superconducting gap structure at the nematic critical point in $FeSe_{1-x}S_x$*, Proc. Natl. Acad. Sci. **115**, 1227 (2018).

[13] T. Hanaguri, K. Iwaya, Y. Kohsaka, T. Machida, T. Watashige, S. Kasahara, T. Shibauchi, Y. Matsuda, *Two distinct superconducting pairing states divided by the nematic end point in $FeSe_{1-x}S_x$*, Sci. Adv. **4**, eaar6419 (2018).

[14] S.J. Kuhn, M. K. Kidder, D. S. Parker, C. dela Cruz, M. A. McGuire, W. M. Chance, L. Li, L. Debeer-Schmitt, J. Ermentrout, K. C. Littrell, M. R. Eskildsen, A. S. Sefat, *Structure and property correlations in FeS*, Physica C **534**, 29 (2017).

[15] X. Yang, Z. Du, G. Du, Q. Gu, H. Lin, D. Fang, H. Yang, X. Zhu, H.-H. Wen, *Strong-coupling superconductivity revealed by scanning tunneling microscope in tetragonal FeS*, Phys. Rev. B **94**, 024521 (2016).

[16] H. Lin, Y. Li, Q. Deng, J. Xing, J. Liu, X. Zhu, H. Yang and H.-H. Wen, *Multiband superconductivity and large anisotropy in FeS crystals*, Phys. Rev. B **93**, 144505 (2016).

[17] J. Xing, H. Lin, Y. Li, S. Li, X. Zhu, H. Yang, H.-H. Wen, *Nodal superconducting gap in tetragonal FeS*, Phys. Rev. B **93**, 104520 (2016).

[18] T. P. Ying, X. F. Lai, X. C. Hong, Y. Xu, L. P. He, J. Zhang, M. X. Wang, Y. J. Yu, F. Q. Huang, and S. Y. Li, *Nodal superconductivity in FeS: Evidence from quasiparticle heat transport*, Phys. Rev. B **94**, 100504(R) (2016).

[19] S. Holenstein, U. Pachmayr, Z. Guguchia, S. Kamusella, R. Khasanov, A. Amato, C. Baines, H.-H. Klauss, E. Morenzoni, D. Johrendt, and H. Luetkens, *Coexistence of low-moment magnetism and superconductivity in tetragonal FeS and suppression of T_c under pressure*, Phys. Rev. B **93**, 140506(R) (2016).

[20] F. K. K. Kirschner, F. Lang, C. V. Topping, P. J. Baker, F. L. Pratt, S. E. Wright, D. N. Woodruff, S. J. Clarke, and S. J. Blundell, *Robustness of superconductivity to competing magnetic phases in tetragonal FeS*, Phys. Rev. B **94**, 134509 (2016).

[21] Y. Yang, W.-S. Wang, H.-Y. Lu, Y.-Y. Xiang, and Q.-H. Wang, *Electronic structure and $d_{x^2-y^2}$-wave superconductivity in FeS*, Phys. Rev. B **93**, 104514 (2016).

[22] X. Lai, Y. Liu, X. Lü, S. Zhang, K. Bu, C. Jin, H. Zhang, J. Lin and F. Huang, *Suppression of superconductivity and structural phase transitions under pressure in tetragonal FeS*, Sci. Rep. **6**, 31077 (2016).

[23] L. Sun, X.-J. Chen, J. Guo, P. Gao, Q.-Z. Huang, H. Wang, M. Fang, X. Chen, G. Chen, Q. Wu, C. Zhang, D. Gu, X. Dong, L. Wang, K. Yang, A. Li, X. Dai, H.-k. Mao and Z. Zhao, *Re-emerging superconductivity at 48 kelvin in iron chalcogenides*, Nature **483**, 67 (2012).

[24] M. Izumi, L. Zheng, Y. Sakai, H. Goto, M. Sakata, Y. Nakamoto, H. L. T. Nguyen, T. Kagayama, K. Shimizu, S. Araki, T. C. Kobayashi, T. Kambe, D. Gu, J. Guo, J. Liu, Y. Li, L. Sun, K. Prassides and Y. Kubozono, *Emergence of double-dome superconductivity in ammoniated metal-doped FeSe*, Sci. Rep. **5**, 9477 (2015).

[25] J.P. Sun, P. Shahi, H. X. Zhou, Y. L. Huang, K. Y. Chen, B. S. Wang, S. L. Ni, N. N. Li, K. Zhang, W. G. Yang, Y. Uwatoko, G. Xing, J. Sun, D. J. Singh, K. Jin, F. Zhou, G. M. Zhang, X. L. Dong, Z. X. Zhao and J.-G. Cheng, *Reemergence of high-Tc superconductivity in the $(Li_{1-x}Fe_x)OHFe_{1-y}Se$ under high pressure*, Nat. Commun. **9**, 380 (2018).

[26] T. Das and C. Panagopoulos, *Two types of superconducting domes in unconventional superconductors*, New J. Phys. **18**, 103033 (2016).

[27] A. R. Lennie, S. A. T. Redfern, P. F. Schofield, D. J. Vaughan, *Synthesis and Rietveld crystal structure refinement of mackinawite*, tetragonal FeS, Mineral. Mag. **59**, 677 (1995).

[28] J. Zhang, F.-L. Liu, T.-P. Ying, N.-N. Li, Y. Xu, L.-P. He, X.-C. Hong, Y.-J. Yu, M.-X. Wang, J. Shen, W.-G. Yang

and S.-Y. Li, *Observation of two superconducting domes under pressure in tetragonal FeS*, npj Quant. Mater. **2**, 49 (2017).

[29] L. Ehm, F. M. Michel, S. M. Antao, C. D. Martin, P. L. Lee, S. D. Shastri, P. J. Chupasc and J. B. Parise, *Structural changes in nanocrystalline mackinawite (FeS) at high pressure*, J. Appl. Crystallogr. **42**, 15 (2008).

[30] K. Koepernik and H. Eschrig, *Full-potential nonorthogonal local-orbital minimum-basis band-structure scheme*, Phys. Rev. B **59**, 1743 (1999); http://www.FPLO.de

[31] J. P. Perdew, K. Burke, and M. Ernzerhof, *Generalized Gradient Approximation Made Simple*, Phys. Rev. Lett. **77**, 3865 (1996).

[32] H. Eschrig and K. Koepernik, *Tight-binding models for the iron-based superconductors*, Phys. Rev. B **80**, 104503 (2009).

[33] M. Tomić, H. O. Jeschke, and R. Valentí, *Unfolding of electronic structure through induced representations of space groups: Application to Fe-based superconductors*, Phys. Rev. B **90**, 195121 (2014).

[34] S. Graser, T. A. Maier, P. J. Hirschfeld, and D. J. Scalapino, *Near-degeneracy of several pairing channels in multiorbital models for the Fe pnictides*, New J. Phys. **11**, 025016 (2009).

[35] See the Supplementary information for details on the crystal structures and the spin fluctuation pairing calculations.

[36] D. Guterding, H. O. Jeschke, P. J. Hirschfeld, and R. Valentí, *Unified picture of the doping dependence of superconducting transition temperatures in alkali metal/ammonia intercalated FeSe*, Phys. Rev. B **91**, 041112(R) (2015).

[37] D. Guterding, *Microscopic modelling of organic and iron-based superconductors*, PhD thesis, Goethe-Universität Frankfurt am Main, Germany (2017).

[38] J. Miao, X. H. Niu, D. F. Xu, Q. Yao, Q. Y. Chen, T. P. Ying, S. Y. Li, Y. F. Fang, J. C. Zhang, S. Ideta, K. Tanaka, B. P. Xie, D. L. Feng, and F. Chen, *Electronic structure of FeS*, Phys. Rev. B **95**, 205127 (2017).

[39] P. Reiss, M. D. Watson, T. K. Kim, A. A. Haghighirad, D. N. Woodruff, M. Bruma, S. J. Clarke, and A. I. Coldea, *Suppression of electronic correlations by chemical pressure from FeSe to FeS*, Phys. Rev. B **96**, 121103(R) (2017).

[40] T. Terashima, N. Kikugawa, H. Lin, X. Zhu, H.-H. Wen, T. Nomoto, K. Suzuki, H. Ikeda and S. Uji, *Upper critical field and quantum oscillations in tetragonal superconducting FeS*, Phys. Rev. B **94**, 100503(R) (2016).

[41] K. Kuroki, H. Usui, S. Onari, R. Arita, and H. Aoki, *Pnictogen height as a possible switch between high-T_c nodeless and low-T_c nodal pairings in the iron-based superconductors*, Phys. Rev. B **79**, 224511 (2009).

Two-dome superconductivity in FeS induced by a Lifshitz transition – Supplemental Material –

Makoto Shimizu,[1] Nayuta Takemori,[1] Daniel Guterding,[2] and Harald O. Jeschke[1,*]

[1] *Research Institute for Interdisciplinary Science, Okayama University, Okayama 700-8530, Japan*
[2] *Institut für Theoretische Physik, Goethe-Universität Frankfurt, Max-von-Laue-Straße 1, 60438 Frankfurt am Main, Germany*

A. Structure

We use the crystal structures for tetragonal FeS ($P\,4/nmm$ space group) as given in Ref. [1]. The structure is defined by a and c lattice parameters and the S height h_S above the iron plane as shown in Figure S1 (a), (b) and (c), respectively. Note that the slightly decreasing height of S above the Fe plane as function of pressure (Figure S1 (c)) translates into a slightly increasing S z fractional coordinate. Relaxation of this position using density functional theory within GGA reverses this trend and is thus unreliable for FeS.

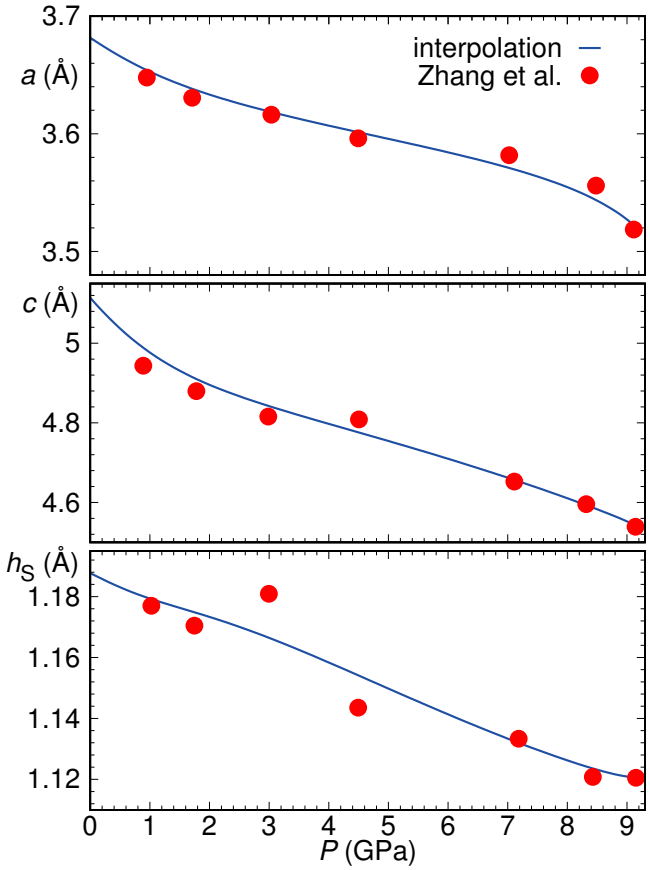

FIG. S1. Experimental crystal structures as measured by Zhang *et al.* [1] (symbols) together with Bézier interpolation (lines). (a), (b) are the tetragonal lattice parameters, and (c) is the height h_S of S above the Fe plane.

* jeschke@okayama-u.ac.jp

B. Origin of the Lifshitz transition

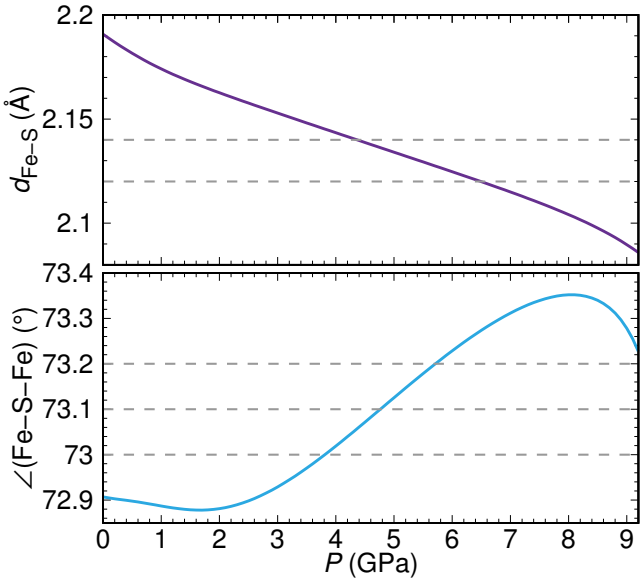

FIG. S2. Variation of (a) Fe-S distance and (b) Fe-S-Fe angle as function of pressure. Dashed lines indicate the bond distances and angles chosen for the plots in Fig. S3.

We investigate which structural change in FeS under pressure is most important for the occurrence of the Lifshitz transition at $P = 4.6$ GPa. Bond length $d_{\text{Fe-S}}$ and $\delta \equiv \measuredangle(\text{Fe-S-Fe})$ in tetragonal FeS are related to lattice constants a and c and sulfur height h_S via

$$\begin{aligned} d_{\text{Fe-S}} &= \sqrt{\frac{a^2}{4} + {h_S}^2} \\ \sin\frac{\delta}{2} &= \frac{a}{2\sqrt{2}d_{\text{Fe-S}}} = \frac{a}{\sqrt{2a^2 + 8{h_S}^2}} \end{aligned} \tag{S1}$$

Figure S2 shows the $d_{\text{Fe-S}}$ and δ calculated for the interpolated series of structures as function of pressure. We now investigate the sensitivity of the electronic structure and in particular the unoccupied band with Fe $3d_{z^2}$ orbital character near the Fermi level to the two relevant structural parameters separately. We focus on structures near $P = 4.6$ GPa. Upon fixing Fe-S distances $d_{\text{Fe-S}}$ and Fe-S-Fe angles δ to the values indicated by the dashed lines in Figure S2, we calculate a lattice parameter and

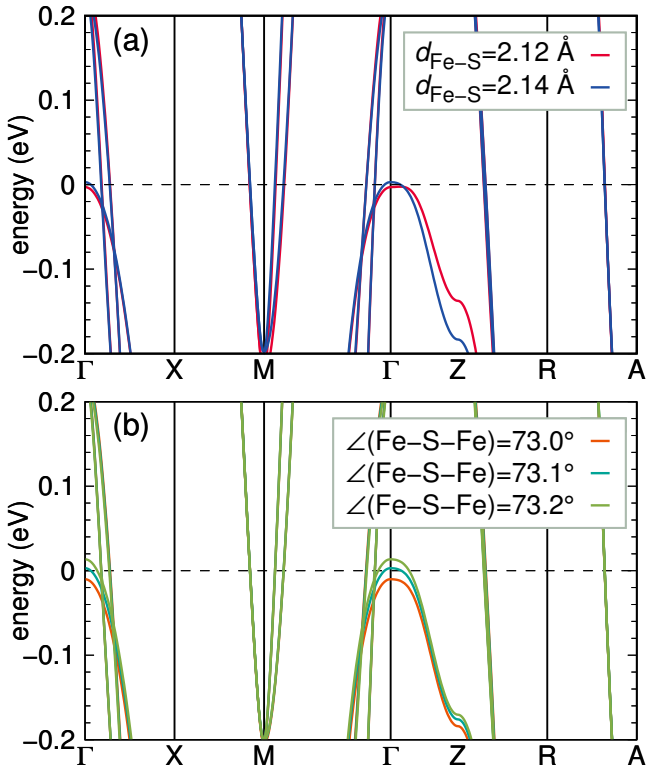

FIG. S3. Change of band structure of FeS for changes in (a) Fe-S distance and (b) Fe-S-Fe angle.

S z coordinate z_{S} by

$$\begin{aligned} a &= 2\sqrt{2} d_{\text{Fe-S}} \sin\frac{\delta}{2} \\ z_{\mathrm{S}} &= \frac{1}{c}\sqrt{{d_{\text{Fe-S}}}^2 - \frac{a^2}{4}} \end{aligned} \tag{S2}$$

Figure S3 shows the result. A very small change in band structure results from the substantial Fe-S bond length change corresponding to a pressure increase of roughly 2 GPa (Figure S3 (a)) once the Fe-S-Fe angle is kept constant; on the other hand, the effect of a pure angle change as is actually relevant in a 2 GPa window leads to a substantial change in band structure (Figure S3 (b)) even if the Fe-S bond lengths are fixed. Thus, the Lifshitz transition can be considered mainly an effect of the deformation of the FeS_4 tetrahedron rather than its pressure induced volume reduction.

C. Spin fluctuation formalism

We follow Graser et al. [2] in considering the multi-orbital Hubbard model

$$\begin{aligned} H = H_0 &+ U\sum_{i,l} n_{il\uparrow} n_{il\downarrow} \\ &+ \frac{U'}{2}\sum_{i,s,p\neq a} n_{is} n_{ip} - \frac{J}{2}\sum_{i,s,p\neq s} \boldsymbol{S}_{is}\cdot\boldsymbol{S}_{ip} \\ &+ \frac{J'}{2}\sum_{i,s,p\neq s,\sigma} c^\dagger_{is\sigma} c^\dagger_{is\bar{\sigma}} c_{ip\bar{\sigma}} c_{ip\sigma} \end{aligned} \tag{S3}$$

where $c^\dagger_{is\sigma}$ ($c_{is\sigma}$) are Fermionic creation (annihilation) operators, $\boldsymbol{S}_{is}$ is the spin operator, $n_{is\sigma} = c^\dagger_{is\sigma} c_{is\sigma}$, U denotes the intraorbital Coulomb repulsion, U' denotes the interorbital Coulomb repulsion, J denotes the Hund's rule coupling and J' denotes the pair-hopping term. The tight binding part of the Hamiltonian is

$$H_0 = -\sum_{i,j} t^{sp}_{ij} c^\dagger_{is\sigma} c_{jp\sigma} \tag{S4}$$

where t_{ij} denotes the transfer integral between sites i and j, s and p are the orbital indices, and σ denotes the spin index. The five band tight binding Hamiltonian is obtained using projective Wannier functions [3] and unfolding [4]. We first calculate the static noninteracting susceptibility

$$\begin{aligned} \chi^{pq}_{st}(\boldsymbol{q}) = -\sum_{\boldsymbol{k},l,m} & a^{p*}_l(\boldsymbol{k}) a^t_l(\boldsymbol{k}) a^{s*}_m(\boldsymbol{k}+\boldsymbol{q}) a^q_m(\boldsymbol{k}+\boldsymbol{q}) \\ & \times \frac{n_F(E_l(\boldsymbol{k})) - n_F(E_m(\boldsymbol{k}+\boldsymbol{q}))}{E_l(\boldsymbol{k}) - E_m(\boldsymbol{k}+\boldsymbol{q})} \end{aligned} \tag{S5}$$

where $E_l(\boldsymbol{k})$ is the energy value determined by the band index l and the wave vector $\boldsymbol{k}$, and $n_F(E)$ is the Fermi distribution function. a^s_m is the matrix element of eigenvectors resulting from diagonalization of tight-binding Hamiltonian H_0. Within the framework of the random phase approximation (RPA) the charge and spin susceptibilities can be calculated from the noninteracting susceptibility

$$\begin{aligned} \left[(\chi^{RPA}_{\mathrm{c}})^{pq}_{st}\right]^{-1} &= \left[\chi^{pq}_{st}\right]^{-1} + (U_{\mathrm{c}})^{pq}_{st} \\ \left[(\chi^{RPA}_{\mathrm{s}})^{pq}_{st}\right]^{-1} &= \left[\chi^{pq}_{st}\right]^{-1} - (U_{\mathrm{s}})^{pq}_{st} \end{aligned} \tag{S6}$$

where the nonzero components of the interaction tensors for the multi-orbital Hubbard model are given by [2]

$$\begin{aligned} (U_{\mathrm{c}})^{aa}_{aa} &= U & (U_{\mathrm{c}})^{aa}_{bb} &= 2U', \\ (U_{\mathrm{c}})^{ab}_{ab} &= \frac{3}{4}J - U' & (U_{\mathrm{c}})^{ba}_{ab} &= J' \\ (U_{\mathrm{s}})^{aa}_{aa} &= U & (U_{\mathrm{s}})^{aa}_{bb} &= \frac{1}{2}J \\ (U_{\mathrm{s}})^{ab}_{ab} &= \frac{1}{4}J + U' & (U_{\mathrm{s}})^{ba}_{ab} &= J', \end{aligned} \tag{S7}$$

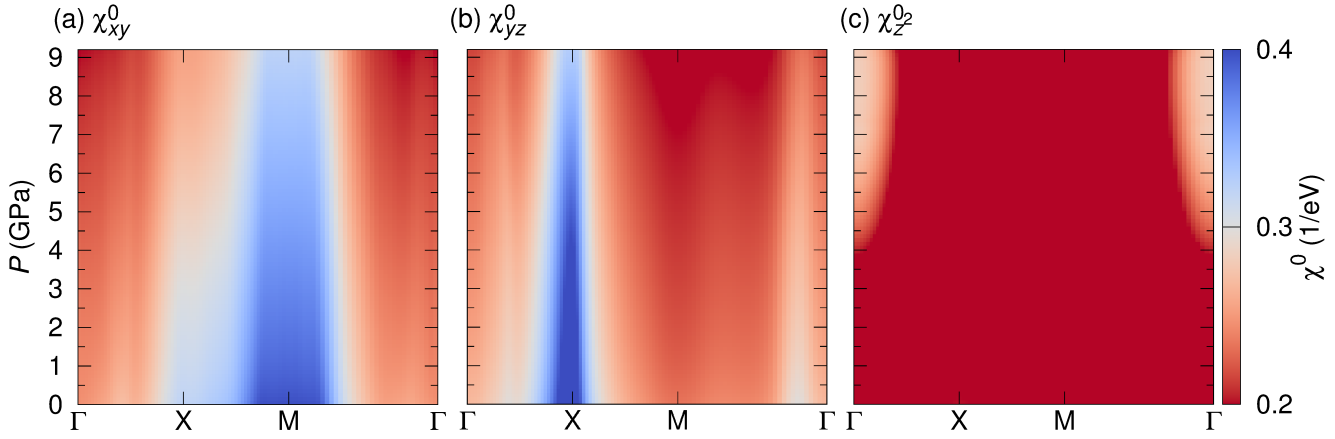

FIG. S4. Pressure dependence of the static noninteracting susceptibility for tetragonal FeS.

which enables us to calculate the two-electron pairing vertex. For the interaction parameters, we find that the choice $U = 1.90$ eV, $U' = U/2$, $J = U/4$ and $J' = U/4$ takes us near the instability for all structures.

Pairing calculations.– The superconducting pairing vertex in the singlet channel is given by

$$\Gamma^{pq}_{st}(\mathbf{k},\mathbf{k}') = \left[\frac{3}{2}U_s\,\chi_s^{RPA}(\mathbf{k}-\mathbf{k}')\,U_s + \frac{1}{2}U_s - \frac{1}{2}U_c\,\chi_c^{RPA}(\mathbf{k}-\mathbf{k}')U_c + \frac{1}{2}U_c\right]^{tq}_{ps}. \tag{S8}$$

The vertex in the orbital space description can be projected onto band space using the eigenvector resulting from diagonalization of the tight-binding Hamiltonian,

$$\Gamma_{ij}(\mathbf{k},\mathbf{k}') = \sum_{s,t,p,q} a_i^{t*}(-\mathbf{k})a_i^{s*}(\mathbf{k})\mathrm{Re}\left[\Gamma^{pq}_{st}(\mathbf{k},\mathbf{k}')\right]a_j^{p}(\mathbf{k}')a_j^{q}(-\mathbf{k}'). \tag{S9}$$

Using the vertex $\Gamma_{ij}(\mathbf{k},\mathbf{k}')$, we solve the gap equation

$$-\sum_j \oint_{C_j}\frac{dk'_{\parallel}}{2\pi}\frac{1}{4\pi v_F(\mathbf{k}')}\left[\Gamma_{ij}(\mathbf{k},\mathbf{k}')+\Gamma_{ij}(\mathbf{k},-\mathbf{k}')\right]g_j(\mathbf{k}') = \lambda_i g_i(\mathbf{k}) \tag{S10}$$

where λ_i denotes the pairing eigenvalue and $g_i(\mathbf{k})$ is the gap function.

D. Noninteracting susceptibility

Figure S4 shows the static noninteracting susceptibilities of FeS for the orbitals that have significant weight at the Fermi level, (a) d_{xy}, (b) d_{yz} (which is by symmetry equivalent to d_{xz} in tetragonal FeS), and (c) d_{z^2}. The latter only acquires features near Γ after the Lifshitz transition because the orbital weight is concentrated on one hole pocket.

E. One-iron Fermi surfaces of FeS

Figure S5 gives the orbital character of FeS Fermi surfaces at two k_z values, $k_z = 0$ and $k_z = \pi$ at ambient pressure and at $P = 5.5$ GPa, after the Lifshitz transition. At $P = 0$, only little $3d_{z^2}$ weight is present in the hole pockets near Γ. The new hole pocket around M has mostly $3d_{z^2}$ character. Comparison of the sizes of the electron pockets around $(\pi, 0, k_z)$ and $(0, \pi, k_z)$ between $k_z = 0$ and $k_z = \pi$ shows that the $P = 5.5$ GPa electronic structure is more three-dimensional than the ambient pressure electronic structure. Three-dimensional susceptibility and pairing calculations are essential for properly describing the pressure dependence of superconductivity in FeS.

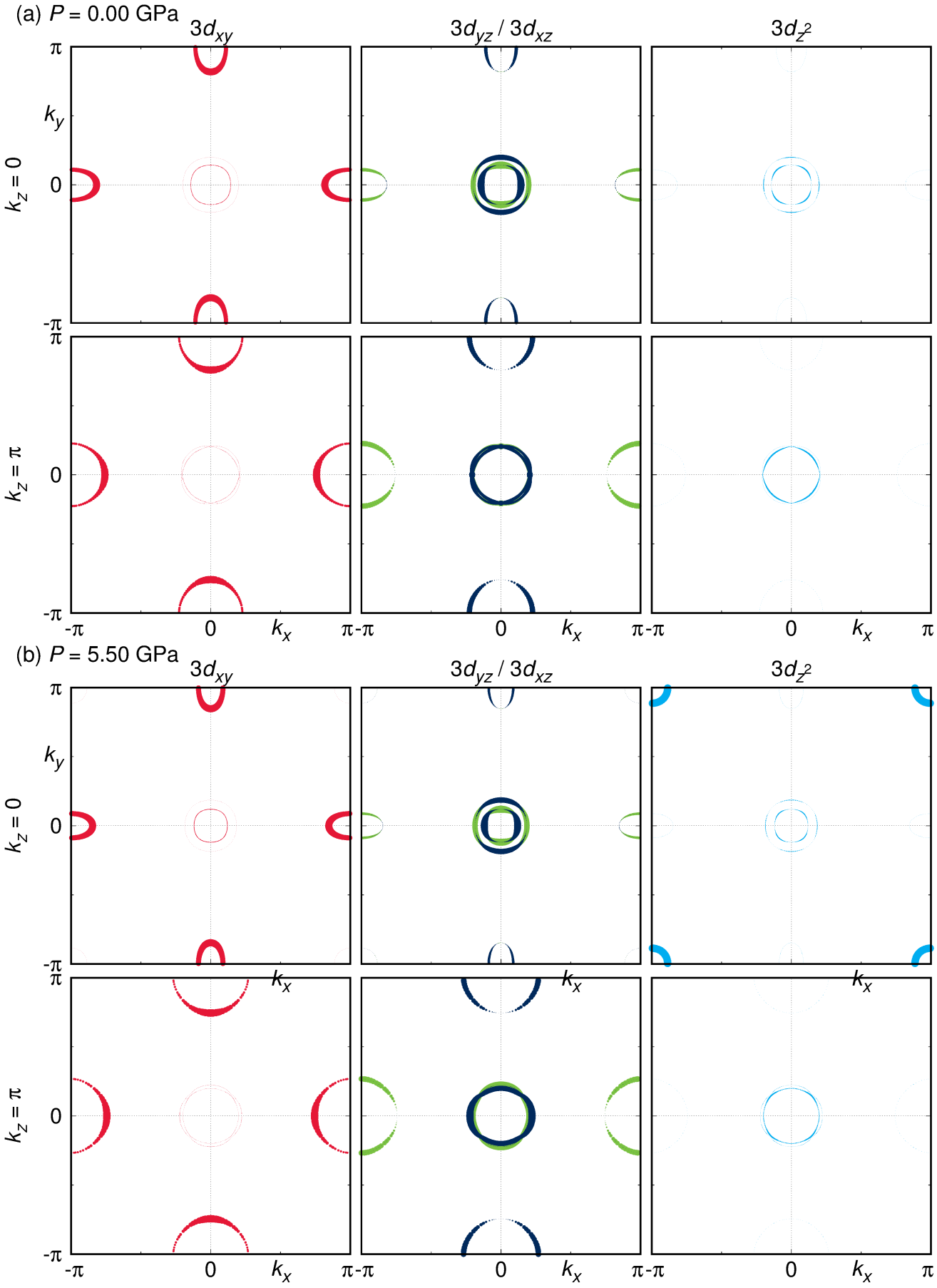

FIG. S5. Fermi surfaces of FeS at two different pressures with orbital weights. They are calculated from the tight binding models which were unfolded to the one-iron Brillouin zone.

F. Off-diagonal components of the spin susceptibility

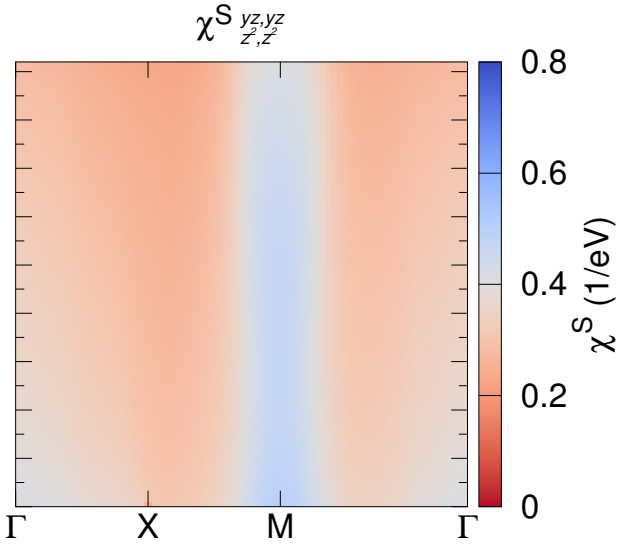

FIG. S6. Pressure dependence of an off-diagonal element of the susceptibility for tetragonal FeS.

Figure S6 shows a relevant off-diagonal component of the spin susceptibility $\chi^{S\,bb}_{\ aa}$ with $a = d_{z^2}$ and $b = d_{yz}$. The even more important off-diagonal component of $\chi^{S\,bb}_{\ aa}$ with $a = d_{z^2}$ and $b = d_{xy}$ is shown in the main text (Figure 2 (d)). $\chi^{S\,bb}_{\ aa}$ with $a = d_{z^2}$ and $b = d_{yz}$ has a weak maximum near $\mathbf{q} = (\pi, \pi)$, due to some nesting between d_{yz}/d_{xz} character hole pockets around Γ and the d_{z^2} character hole pocket around M.

G. Solution of the gap equation with intra-orbital interaction only

In Figure S7, we demonstrate the effect of inter-orbital interaction terms by determining the solution of the gap equation at $U' = J = J' = 0$. The solution at $P = 4.7$ GPa (and higher pressures) is a simple nodeless sign-changing s-wave instead of the more complicated $s_\pm$ solution shown in Figure 3 (c) of the main text.

It arises from the $\mathbf{q} = (\pi, 0), (0, \pi)$ nesting of the d_{yz}/d_{xz} orbitals. Note also the remaining orbital weight of d_{xy} and d_{z^2} around Γ in Figs. 3(a) and (c) of the main text, which enables these orbitals to participate in a $s_\pm$ solution.

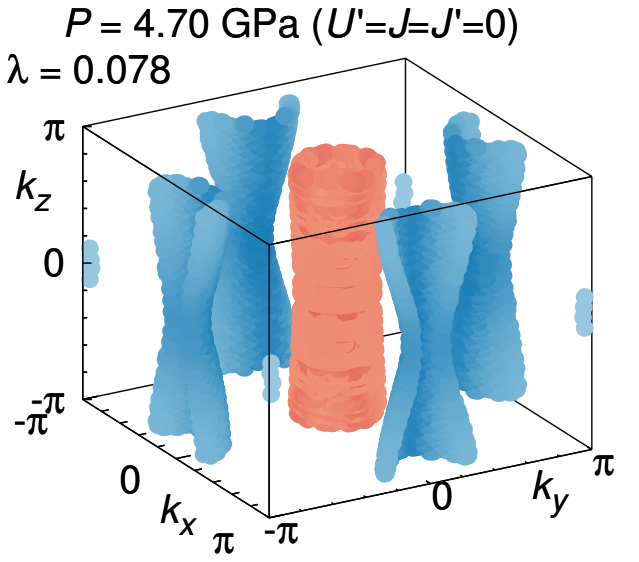

FIG. S7. Hypothetical leading gap function for FeS at $P = 4.7$ GPa for $U = 1.9$ eV and $U' = J = J' = 0$. The three-dimensional Fermi surface is plotted in the one-iron Brillouin zone.

[1] J. Zhang, F.-L. Liu, T.-P. Ying, N.-N. Li, Y. Xu, L.-P. He, X.-C. Hong, Y.-J. Yu, M.-X. Wang, J. Shen, W.-G. Yang and S.-Y. Li, Observation of two superconducting domes under pressure in tetragonal FeS, npj Quant. Mater. **2**, 49 (2017).

[2] S. Graser, T. A. Maier, P. J. Hirschfeld, and D. J. Scalapino, Near-degeneracy of several pairing channels in multiorbital models for the Fe pnictides, New J. Phys. **11**, 025016 (2009).

[3] H. Eschrig and K. Koepernik, Tight-binding models for the iron-based superconductors, Phys. Rev. B **80**, 104503 (2009).

[4] M. Tomić, H. O. Jeschke, and R. Valentí, Unfolding of electronic structure through induced representations of space groups: Application to Fe-based superconductors, Phys. Rev. B **90**, 195121 (2014).